AIP | Conference Proceedings

Validation of an optical model applied to the beam down CSP facility at the Masdar Institute Solar Platform

Benjamin Grange, Vikas Kumar, Juliana Beltran Torres, Victor G. Perez, Peter R. Armstrong, Alexander Slocum, and Nicolas Calvet

---

Articles you may be interested in

The Masdar Institute solar platform: A new research facility in the UAE for development of CSP components and thermal energy storage systems
AIP Conf. Proc. **1734**, 100003 (2016); 10.1063/1.4949191

Validation of Cosmic Ray Ionization Model CORIMIA applied for solar energetic particles and Anomalous Cosmic Rays
AIP Conf. Proc. **1714**, 040001 (2016); 10.1063/1.4942575

Experimental validation of adding-doubling modeling of solar cells including luminescent down-shifting layers
J. Renewable Sustainable Energy **7**, 043130 (2015); 10.1063/1.4928874

SU-E-T-36: A GPU-Accelerated Monte-Carlo Dose Calculation Platform and Its Application Toward Validating a ViewRay Beam Model
Med. Phys. **42**, 3339 (2015); 10.1118/1.4924397

OTR Measurements and Modeling of the Electron Beam Optics at the E-Cooling Facility
AIP Conf. Proc. **821**, 380 (2006); 10.1063/1.2190139

Validation of an Optical Model Applied to the Beam Down CSP Facility at the Masdar Institute Solar Platform

Benjamin Grange [1, a)], Vikas Kumar [1], Juliana Beltran Torres [1], Victor G. Perez [1], Peter R. Armstrong [1], Alexander Slocum [2], and Nicolas Calvet [1, b)]

[1] *Institute Center for Energy, Department of Mechanical and Materials Engineering,*
Masdar Institute of Science and Technology, Masdar City, P.O. Box 54224, Abu Dhabi, United Arab Emirates.
[2] *Department of Mechanical Engineering,*
Massachusetts Institute of Technology, 77 Massachusetts Ave, Cambridge, MA 02139, United States of America.

a) Corresponding author, Postdoctoral Researcher, bgrange@masdar.ac.ae
b) Assistant Professor, ncalvet@masdar.ac.ae

Abstract. In the framework of the CSPonD Demo project, the optical characterization of the Beam Down Optical Experiment (BDOE) heliostats field is an important step to certify the required power is provided. To achieve this goal, an experiment involving a single heliostat is carried out. The results of the experiment and the comparison with simulated results are presented in this paper. Only the reflection on the heliostat is observed in order to have a better assessment of its optical performance. The heliostat reflectance is modified and the experimental and simulated concentration distribution are confronted. Results indicate that the shapes of the concentration distributions are quite similar, hence validating the optical model respects the geometry of the BDOE. Moreover these results lead to an increase of the optimized heliostat reflectance when the incident angle on the heliostat decreases. Further investigation is required to validate this method with all the individual heliostats of the BDOE solar field.

INTRODUCTION

The CSPonD Demo (Concentrated Solar Power on Demand Demonstration) project[1] involves design and testing of a molten salt tank, which acts simultaneously as the solar receiver and thermal energy storage. This tank is being tested under concentrated solar flux of the Beam Down Optical Experiment (BDOE) at the Masdar Institute Solar Platform (MISP). A final optical element (FOE) is also implemented to further increase the concentration ratio while reducing the tank aperture, hence reducing thermal losses[2]. The prediction of incident solar radiation is essential to optimize the FOE and balance of the optical system. Following the work of Mokhtar et al.[3], an optical model[4] has been developed to analyze the BDOE and FOE performance. As a first step to validate the optical model, this paper focuses on the optical performance after the reflection on each heliostat (HS). Experimental and simulated concentration distributions at the top of the tower are compared.

THE BEAM DOWN OPTICAL EXPERIMENT

The BDOE at the Masdar Institute Solar Platform is a point focus Fresnel concentrator with a primary reflective surface of 280 m^2. The heliostats collect and concentrate solar beam radiation toward an upper focal point, as shown in Figure 1(a). Between the heliostats and the upper focal point, a set of flat central reflector (CR) facets approximating a hyperbolic profile are tilted to redirect the radiation downward onto the receiver aperture situated near the ground.
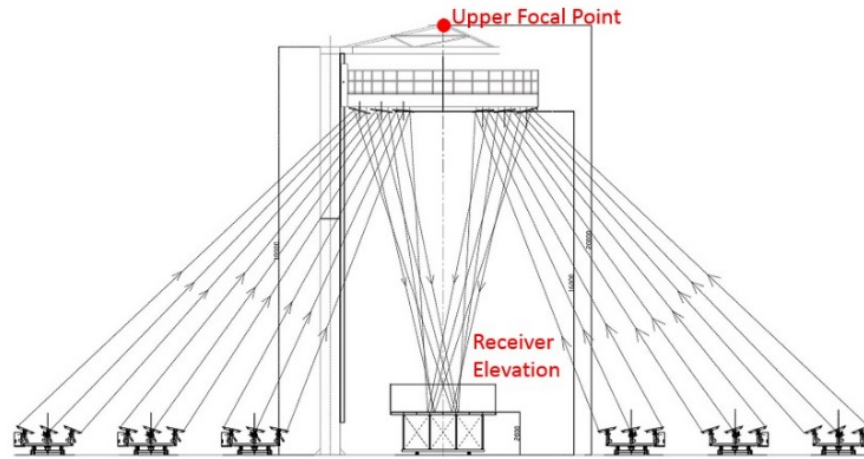
(a)
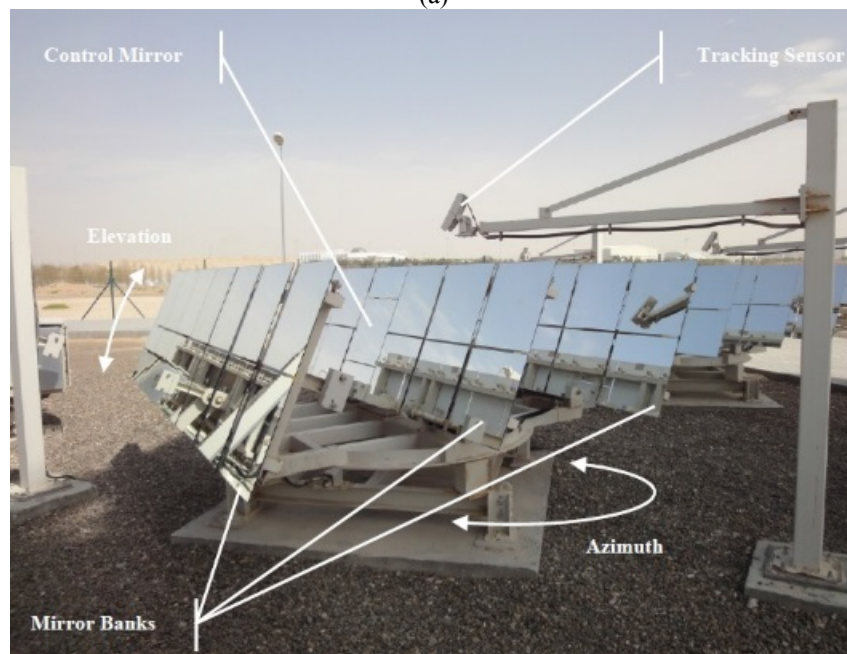
(b)

FIGURE 1. (a) Vertical cross sectional view of the BDOE; (b) Picture of one heliostat.

Each gang-type heliostat consists of 43 flat facets arranged in three banks as shown in Figure 1(b). In addition to the heliostat facets' canting, the front and back banks are tilted with respect to the middle one. Canting errors of the facet can lead to different optical performance of the heliostats, which is analyzed in this paper.

Three focal lengths, corresponding to the three rings of heliostats (cf. Figure 2), are shorter than the path to the bottom target plane. This feature results from a trade-off between the size of the central reflector mirrors and the concentration level on the target. However in the CSPonD Demo project[1], the concentration ratio achieved by the BDOE is increased by positioning the inlet aperture of the FOE higher than the receiver inlet plane. With this new receiver and FOE concept, an optical model must be developed optimize the FOE design and maximize the incident power at the FOE outlet. In this paper we describe the experimental method used to check fidelity of the optical model and present the initial results of model validation.
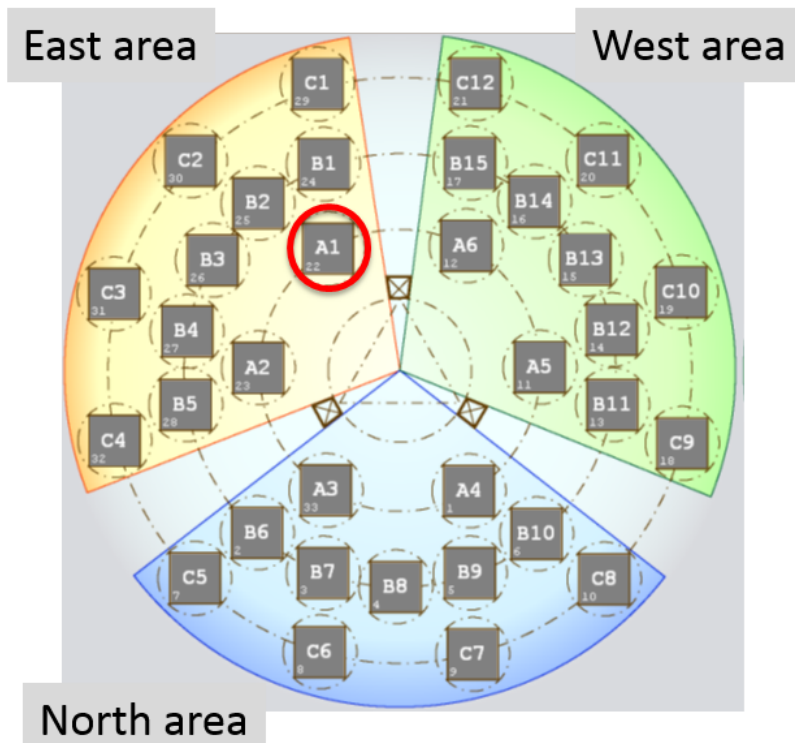
FIGURE 2. Heliostats field layout.

OPTICAL ANALYSIS

Optical Model

TracePro™ is used to estimate the flux distribution provided by each heliostat. This software is a ray tracing program for optical analysis of solid models first developed under a NASA SBIR contract. TracePro™ traces rays using "Generalized Ray Tracing". At each intersection, individual rays can be subject to absorption, reflection, refraction, diffraction and scatter[5]. It is chosen mostly because of its built-in Compound Parabolic Concentrator (CPC) and cone objects (convenient for the CSPonD Demo project), as well as its use of a very general modeling language. All the input data (heliostat/CR coordinates and layout, receiver position, sun position and Direct Normal Irradiation) are processed in a Matlab™ code that generates a complete geometry description executable by TracePro™. Optical properties are applied (specularity, reflectivity, etc.) and a Monte-Carlo ray-tracing is launched.

Experimental Set Up

The experiment is based on an indirect measurement associated to a direct measurement[6]. A Charge-Coupled Device (CCD) camera facing up towards the upper focal point is set up on the moveable CR platform and operated with the platform in the position shown in Figure 3(c). Facing down is a lambertian target installed 30 cm below the upper focal point. Four heat flux sensors (HFS) are installed on the target to calibrate the CCD pictures and assess the lambertian property of the target. The first HFS is located in the center of the target while the three others are located 25 cm from the center towards the North, the South-West and the South-East directions.

To carry out the experiment while focusing a single heliostat, the CR platform of the BDOE must be brought down, as shown from Figures 3(a) to 3(b).
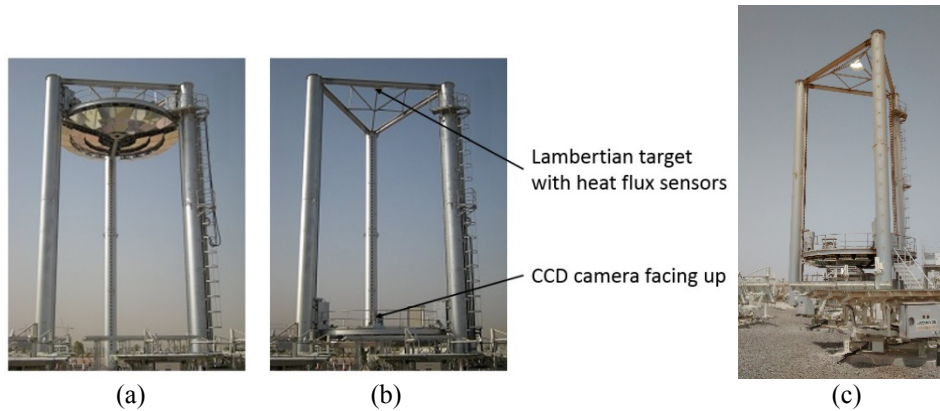
FIGURE 3. CR platform shown in normal position (a), lowered for the experiment (b) and with a heliostat tracking the sun (c).

A CCD picture consists of three different signals:

- The photon signal: a portion of the photons coming from the white target to the CCD sensor is converted into electrons. The camera delivers numerical data proportional to the amount of electrons measured for each pixel.
- The thermal signal: molecular agitation in the CCD sensor leads to the creation of electrons of thermal origin, hence there is mixing with electrons of luminous origin.
- The luminous offset: the CCD camera gives a low-intensity value for a null luminous intensity. This value depends on the design of the camera and the electronic tuning carried out in the factory.

Offsets are present in all these signals. Therefore the signals are pre-processed, by subtracting a background CCD picture (white target without the solar flux distribution) from the CCD picture obtained with the heliostat under test. Both CCD pictures must be taken in close temporal succession under the same conditions of ND filter, exposure time, and steady sky/DNI conditions.

The conversion in a concentration ratio distribution is chosen to normalize the distribution in order to compare the optical performance of the heliostat without any influence of the Direct Normal Radiation (DNI). It is achieved by calculating an average value of the intensity around each HFS. This value is compared with the concentration ratio provided by each HFS (flux density divided by DNI).

To erase the disruptions created by the HFS on the CCD picture, the intensity of the HFS pixels is assumed to be equal to the average of pixel values around it.

RESULTS

The results focus on the optical performance of one heliostat, A1, located in the South-East part of the field (surrounded in red in Figure 2). Experimental concentration distributions, for three different times of the day, are compared with the simulated concentration distributions delivered by the ray tracing software.

Figure 4(a) shows the CCD picture corresponding to heliostat A1 at 10 AM (local time in Abu Dhabi) the 15th of July 2015, while Figure 4(b) presents the same picture after conversion in concentration, for a mesh dimension of 5 cm x 5 cm.
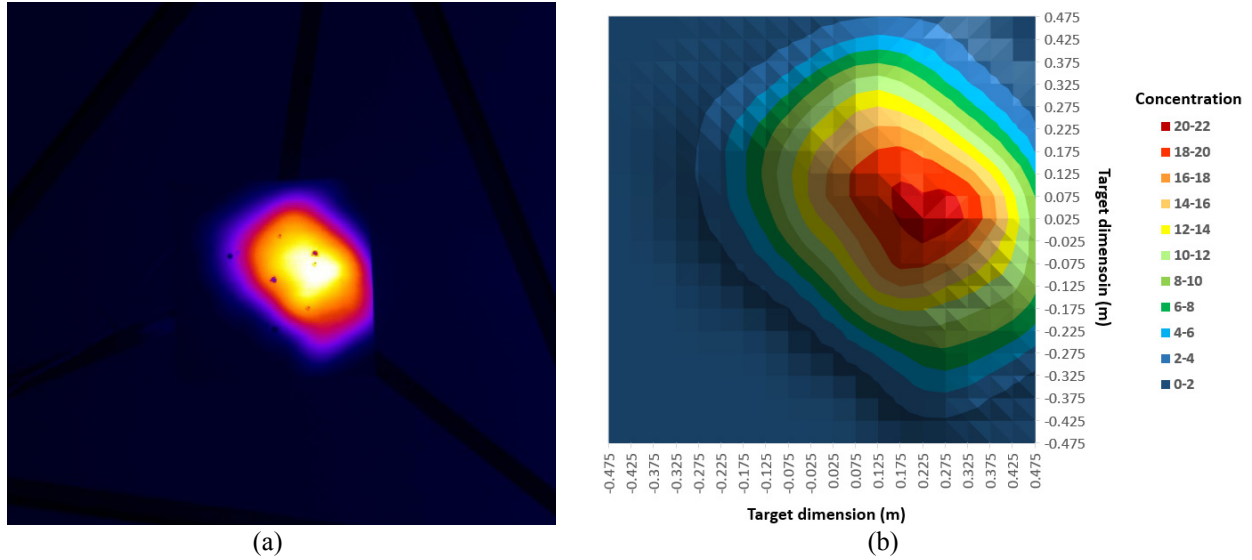
FIGURE 4. (a) CCD picture of A1 at 10 AM the 15th of July 2015, local time in Abu Dhabi; (b) Conversion of the CCD picture in concentration density for a mesh dimension of 5 cm x 5 cm.

With the protective front glass layer on the heliostat, the reflectivity changes with regard to the incident angle. Therefore simulated concentration distributions for different heliostat reflectance, with and without taking into account the facets' canting errors, are obtained with the ray-tracing software. The cumulative distribution of the facets' canting errors is shown in Figure 5 and is based on measurements made in 2009[7].
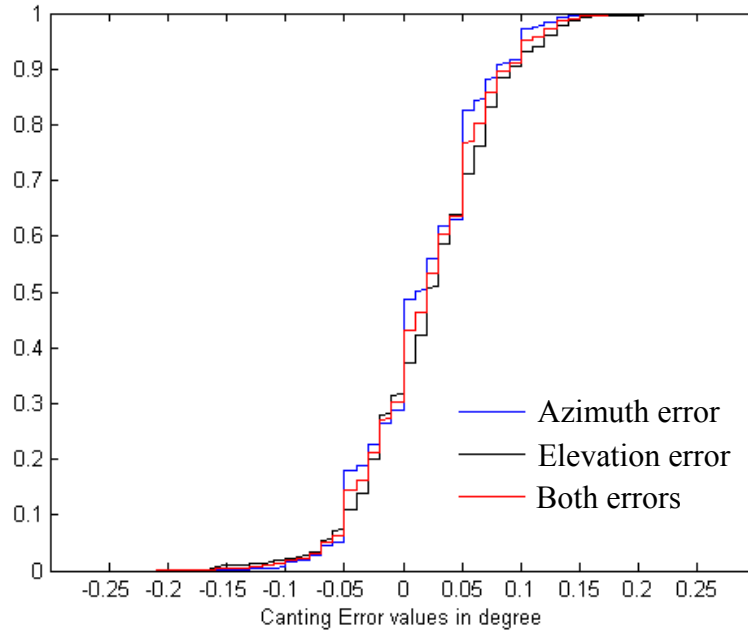

FIGURE 5. Cumulative distribution of facets' canting errors in degrees (measurement made on 1419 facets).

To compare the simulated and experimental concentration distributions, two parameters are defined. The first parameter is the relative difference of the maximum concentration ratio in the meshes ΔC_{rel}:

$$\Delta C_{rel} = \frac{C_{exp}^{max} - C_{sim}^{max}}{C_{exp}^{max}} \times 100 \qquad (\%) \qquad (1)$$

Where C_{exp}^{max} (-) and C_{sim}^{max} (-) are the maximum concentrations in the experimental and simulated distributions, respectively.

The second parameter is the relative standard deviation of concentration difference per mesh σ_{rel}:

$$\sigma_{rel} = \frac{\sqrt{\frac{1}{n-1}\sum_{i=1}^{n}\left(\Delta C^i - \overline{\Delta C}\right)^2}}{\overline{C_{exp}}} \times 100 \qquad (\%) \qquad (2)$$

Where n is the index of the surface mesh element, $\overline{C_{exp}}$ is the average experimental concentration ratio in the meshes (-) and $\overline{\Delta C}$ the average difference of the concentration ratio per mesh between the experimental and the simulated distributions:

$$\overline{\Delta C} = \frac{1}{n}\sum_{i=1}^{n}\left(C_{exp}^i - C_{sim}^i\right) \qquad (-) \qquad (3)$$

The relative standard deviation is a parameter that represents the accuracy of the numerical concentration distribution compared to the experimental one.

Figure 6 shows the evolution of the relative standard deviation as a function of the heliostat reflectance, for three different time, with and without considering the facets' canting error. A large range of heliostat reflectance is covered (from 50 % to 90 %) for two reasons: the first one is in the case of a heliostat that hasn't been cleaned, the second is to emphasize the optimal (minimum) relative standard deviation.
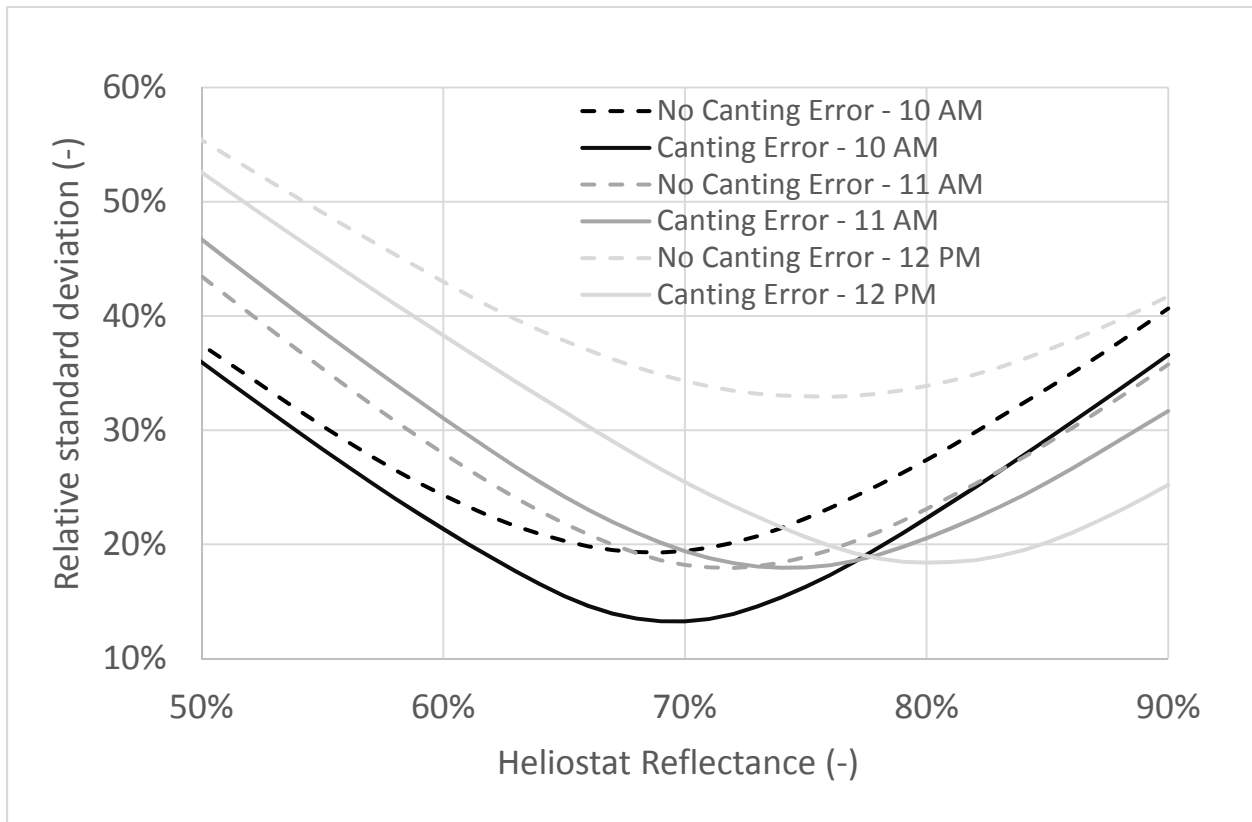

FIGURE 6. Evolution of the relative standard deviation as a function of the heliostat reflectance – A1 at 10 AM, 11 AM and 12 PM the 15th of July – Without and with facets' canting error.

These results reveal that taking into account the facets' canting errors allows to reduce the comparison criterion. Moreover the increase of the optimal heliostat reflectance from 10 AM to 12 PM is consistent with the decrease of

the incident angle on the heliostat (less absorption in the protective front glass layer). Table 1 sums up the optimal values obtained in this optical analysis.

Time	Optimal heliostat reflectance	σ_{rel} (-)	ΔC_{rel} (-)
10 AM	70 %	13.3 %	- 4.6 %
11 AM	74 %	17.9 %	- 1.2 %
12 PM	80 %	18.4 %	10.1 %

As the analysis with facets' canting errors is more conclusive, Figures 8 and 9 present the corrected experimental concentration distribution and the simulated concentration distribution of heliostat A1 the 15th of July 2015 at 11 AM and at 12 PM, respectively.
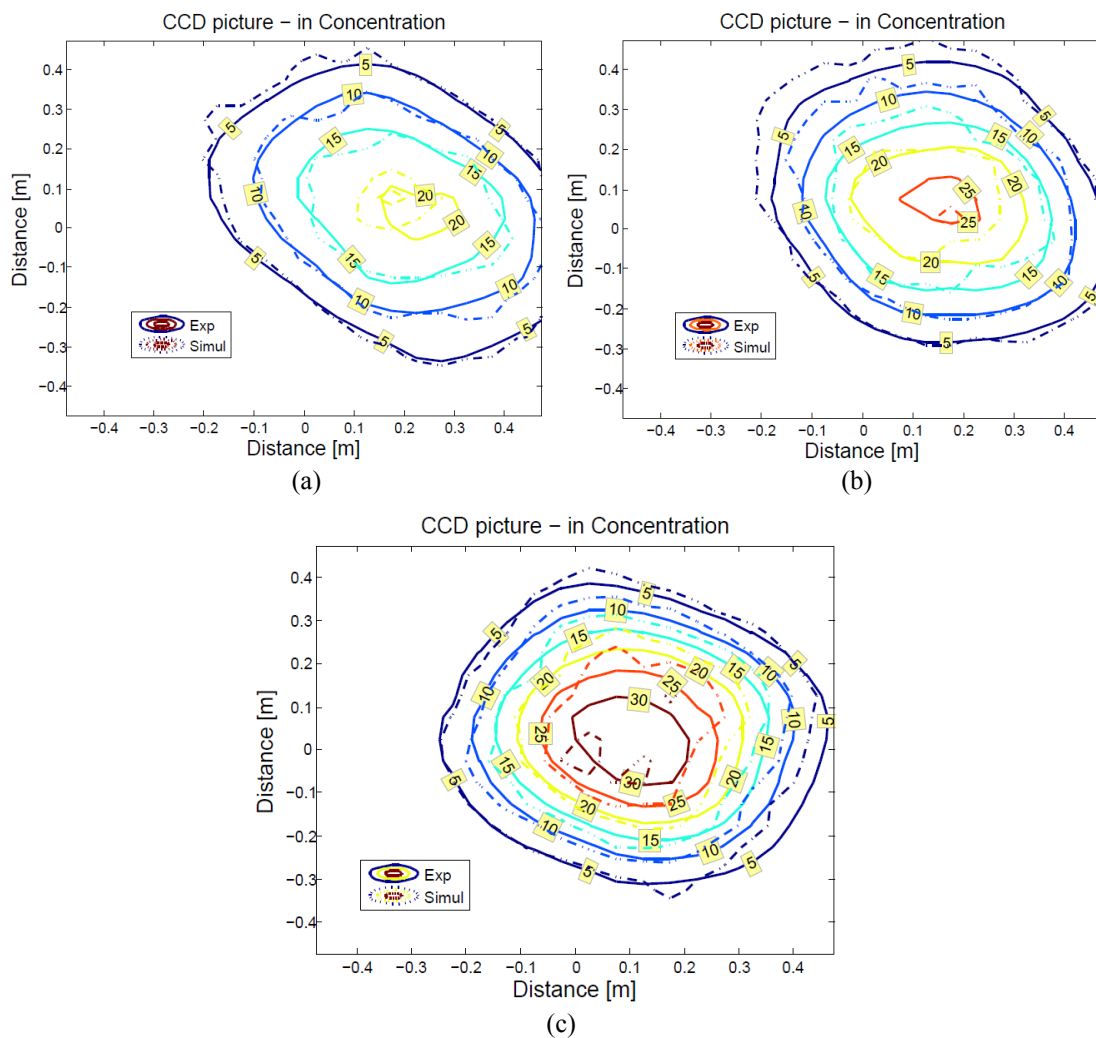

FIGURE 7. Comparison of experimental and optimized simulated concentration distributions –

(a) 10 AM (b) 11 AM and (c) 12 PM

CONCLUSION AND DISCUSSION

Although several individual heliostat flux distributions have been observed, this paper presents the optical performance of one heliostat of the Masdar Institute Solar Platform heliostats field, and the comparison with the simulated concentration distribution. Although we had some spillage due to the target location 30 cm below the focal point, first results on heliostat A1 show a good agreement between simulated and experimental concentration distributions.

With the 4 HFS installed on the target, a first analysis reveals the accuracy of the HFS measurements associated to the signal of the CCD camera surrounding the HFS. Relative standard deviations (corresponding to the standard deviation over the mean value) of the 4 conversion factors are calculated for the three experimental pictures and give 3.6 %, 5.8 % and 7.2 % at 10 AM, 11 AM and 12 PM, respectively. The increase of the relative standard deviation from 10 AM to 12 PM might be due to a disruption of the signal of the CCD camera while the sun is reaching its zenith. This analysis revealed that the facet's canting errors must be taken into account to obtain simulated concentration distributions closer to the experimental ones. Finally the shape of the experimental and simulated concentration distributions are rather similar which indicates that the model developed in TracePro™ represents the geometry of the BDOE at the Masdar Institute Solar Platform with reasonable fidelity.

PERSPECTIVES

Additional experiments are required to analyze all individual heliostats of the MISP field. The alignment of the solar sensor will be modified to aim at the center of the white target and be able to obtain the whole concentration distribution on it. These concentration distributions will be confronted to the simulated ones in order to analyze the optical performance of each heliostats after several years. Understanding their optical behavior will allow to enhance their optical efficiency, hence obtaining higher incident flux for the CSPonD Demo project.

A special paint or coating, such as a plasma-sprayed Al_2O_3, must be applied on the target to produce nearly lambertian behavior. Finally a larger target will be installed to be able to observe the entire concentration map.

ACKNOWLEDGEMENTS

REFERENCES

1. A. H. Slocum, D. S. Codd, J. Buongiorno, C. Forsberg, T. McKrell, J.-C. Nave, C. N. Papanicolas, A. Ghobeity, C. J. Noone, S. Passerini, F. Rojas, A. Mitsos, Solar Energy **85** (7), 1519-1529 (2011).
2. B. Grange, V. Kumar, A. Gil, P. R. Armstrong, D. S. Codd, A. Slocum and N. Calvet, in *International Conference on Applied Energy ICAE 2015* (Energy Procedia, Abu Dhabi, UAE, 2015).
3. M. Mokhtar, S.A. Meyers, P.R. Armstrong, M. Chiesa, J. of Sol. Energy Eng. **136** (4), 4-8 (2014).
4. V. Kumar, "Modeling of Beam Down Solar Concentrator and Final Optical Element Design," M.Sc. thesis, Masdar Institute of Science and Technology, 2015.
5. R. Dovesi, V. R. Saunders, C. Roetti, R. Orlando, F. Pascale, B. Civalleri, K. Doll, N. M. Harrison, I. J. Bush, P. D. Arco, M. Llunel, and M. Caus, *TracePro75 User's Manual* (2014).
6. M. Röger, P. Hermann, S. Ulmer, M. Ebert, C. Prahl, F. Göhring, J. of Sol Energy Eng, **136** (3), 1-10 (2014).
7. MES, "Inspection Plan Beam Down Solar Concentration System," HJR001 (2009).